Journal of ELECTRICAL ENGINEERING, VOL 61. NO 7/s, 2010, 89-92

COMPARISONS OF AC MAGNETOSTRICTION OF NON-ORIENTED ELECTRICAL STEELS MEASURED IN EPSTEIN AND DISC SAMPLES

Sakda Somkun* ─ Piotr Klimczyk ─ Anthony J. Moses ─ Philip I. Anderson

Magnetostriction data of non-oriented electrical steel is needed for calculation of deformation and vibration of electrical machine cores. It is characterised on various sample shapes using several measurement techniques which may give different results. In this paper, measurement results of AC magnetostriction of two commercial non-oriented steels magnetised at angles to the rolling direction in standard Epstein strip and disc samples are presented. Magnetostriction measured in disc samples magnetised in a two-dimensional magnetisation system revealed that the highest magnetostriction in the sheet plane may not occur along the magnetisation direction if the material is anisotropic. Sample geometry also caused differences of magnetostriction measured in the Epstein and disc samples due to the form effect. The results show that magnetostriction measured in Epstein strip form should be used with caution for calculation of core deformation and vibration of large electrical machines.

Keywords: anisotropy, electrical steel, magnetostriction, rotational magnetisation

1 INTRODUCTION

Magnetostriction (λ) of non-oriented (NO) electrical steel, commonly used in electrical machine cores, is a source of stator core deformation and vibration [1]. It has been reported that magnetostriction in some grades of NO steel is more anisotropic than its specific power loss [2]. This magnetostrictive anisotropy of NO steel can create asymmetrical deformation around an AC machine stator core [3]. Anisotropy characteristics of magnetic properties of electrical steel are conventionally characterised in Epstein strips cut at angles (θ) to the rolling direction (RD) and magnetised along the sample length. This is time consuming and a waste of expensive material. Anisotropy can be alternatively assessed using square or disc samples magnetised in a two-dimensional (2D) magnetisation system [4]. Magnetic characteristics of grain-oriented (GO) electrical steel have been reported to be affected by the geometry-dependent demagnetisation factor [5]. Hence, this could cause differences in magnetostriction of NO steel measured in various sample shapes. This paper reports the angular characteristics of two NO steels measured in Epstein strips and disc samples.

2 EXPERIMENTAL APPROACH

2.1 Sample preparation

Two grades of commercial NO steels were chosen as listed in Table 1. Their percentage silicon contents were estimated from the nominal densities. Standard Epstein strips (305 mm long 30 mm wide) of the 0.50 mm thick steel were cut from a batch of square sheets, 400 mm × 400 mm at 10° intervals from the RD to the transverse direction (TD) using an electric-powered guillotine with a sharp blade. Three strips were cut at each angle. No heat treatment is required for Epstein samples of NO steel delivered in the finally annealed state material, except those used in aging tests [6]. Although the plastic and elastic stresses close to the cut edges of the strips were present, this was assumed to be consistent from sample to sample because of the same shearing force provided by the electric-powered guillotine.

Two Epstein samples of the 0.35 mm thick steel were cut from a 500 mm × 500 mm sheet along the RD and TD by electric discharge machining. These samples were initially used for a comparison of effects of cutting techniques on magnetostriction carried out by Klimczyk [7]. The samples were annealed in a nitrogen atmosphere at a temperature of 800° C for 2 hours.

Each material was also cut into an 80 mm disc sample and four 0.50 mm holes were drilled at the centre of each for 20 mm long orthogonal *b* coils. The 0.35 mm and 0.50 mm disc samples and the 0.35 mm thick Epstein samples were annealed in a nitrogen atmosphere at a temperature of 800° C for 2 hours to release stresses due to cutting and drilling.

Table 1. Physical properties of NO samples

Nominal thickness (mm)	Nominal density (kg/dm^3])	Estimated Silicon Contents (%)
0.50	7.70	2.5
0.35	7.60	4.0

2.2 AC magnetostriction measured on Epstein samples

The Epstein strips were magnetised singly under sinusoidal induction at peak flux density ($\hat{B}$) from 1.00 T to 1.70 T ± 0.005 T, 50 Hz in an AC magnetostriction measurement system [8]. One end of the strip was clamped and no longitudinal stress was applied. Peak to peak values of magnetostriction ($\lambda_{MD_{PP}}$) along the magnetisation direction (MD) were obtained by double integration of the output signal of an accelerometer fixed at the free end of the strip. Thus, the initial constant of the double integration could be neglected. Repeatability test of each strip was carried out 3 times and the expanded uncertainty of over the above flux density range without stress applied, was estimated to be within ± 5 %.

* Wolfson Centre for Magnetics, Cardiff School of Engineering, Cardiff University, United Kingdom, SomkunS@Cardiff.ac.uk

ISSN 1335-3632

2.3 AC magnetostriction measured on disc samples

Rectangular rosette foil resistance strain gauges were attached at the centre of each disc as shown in Fig 1 (a). Each 6 mm long gauge had a resistance of 120 ± 0.5 Ω and gauge factor of 2.10 ± 1%. Each was connected in a half bridge configuration with a dummy gauge for temperature compensation [9]. Instantaneous flux density components along the RD and TD (b_x and b_y) were calculated from the voltages induced in the orthogonal b coils. The samples were magnetised in a two-phase stator core shown in Fig. 1 (b).

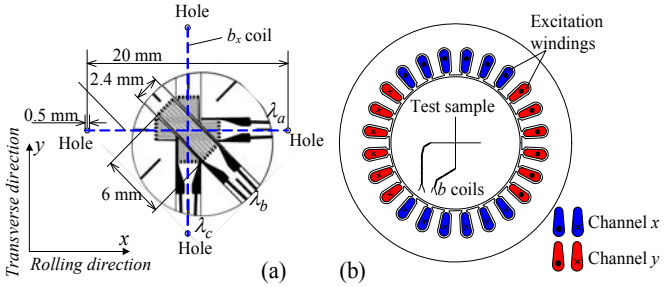

Fig. 1. (a) - Locations of rosette resistance strain gauges and orthogonal b coils at the centre of a disc sample, (b) -Schematic diagram of a disc sample placed in a magnetising yoke of the 2D magnetisation system

b_x and b_y were controlled independently in a LabVIEW program to create a net alternating magnetisation at angle θ with respect to the RD as shown in Fig. 2 (a). Three measured magnetostrictive strains λ_a, λ_b and λ_c were transformed to magnetostriction components along the RD and TD (λ_{RD} and λ_{TD}) and a shear magnetostriction component between the RD and TD (λ_{TD}). Thus, the arbitrary in-plane magnetostriction at angle φ with respect to the RD can be written as

$$\lambda(\varphi,t) = \lambda_{RD}(t)\cos^2\varphi + \lambda_{TD}(t)\sin^2\varphi + \gamma_{RT}(t)\sin\varphi\cos\varphi \qquad (1)$$

Magnetostriction along the MD is obtained by setting $\varphi = \theta$ in (1). The principal axis of magnetostriction may not occur along the MD as illustrated in Fig. 2 (b). The maximum elongation (λ_1) and contraction (λ_2) are then calculated from

$$\lambda_1, \lambda_2 = \frac{\lambda_{RD} + \lambda_{TD}}{2} \pm \sqrt{\left(\frac{\lambda_{RD} - \lambda_{TD}}{2}\right)^2 + \left(\frac{\gamma_{RT}}{2}\right)^2}. \qquad (2)$$

This experiment setup is described in detail in [10]. Each disc was magnetised over the induction range of 0.50 T to 1.80 T, 50 Hz and $\theta = 0°$ to 90° at 10° intervals. Each magnetisation condition was averaged over 50 magnetisation cycles to reduce any effect of random noises. Each was repeated five times. The expanded uncertainties of flux density and magnetostriction measurements of this system were evaluated to be ± 2 % and ± 12 % respectively.

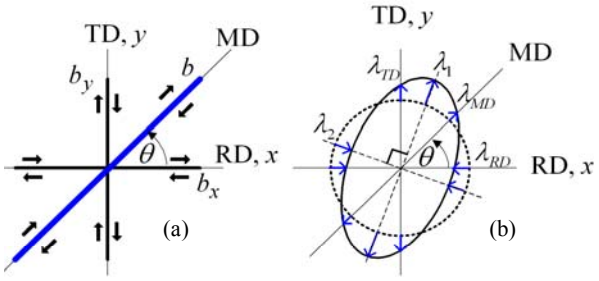

Fig. 2. (a) -Vector depicting alternating magnetisation applied to disc samples, (b) - Illustration of magnetostriction components in disc samples

3 RESULTS

Figure 3(a) and (b) show deformation plots of the 0.35 mm and 0.50 mm disc samples at b=1.70 T and $\theta = 40°$. It can be observed that the principal axis of the 0.50 mm thick steel is far away from MD. Therefore, its λ_{MD} does not represent the maximum magnetostriction occuring in the sheet plane.

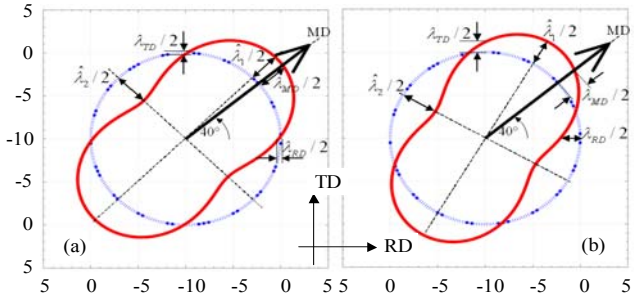

Fig.3. Magnetostriction components of (a) the 0.35 mm thick disc sample and (b) the 0.50 mm thick disc sample both at 1.70 T and θ=40°

$\lambda_{MD_{PP}}$ and peak values of λ_1 and λ_2 ($\hat{\lambda}_1$ and $\hat{\lambda}_2$) measured in the 0.35 mm and 0.50 mm thick disc samples at $\hat{B}$ =1.50 T are shown in Fig. 4 and Fig. 5 respectively. $\lambda_{MD_{PP}}$ and $\hat{\lambda}_1$ of the 0.35 mm thick material are almost the same because its principal axis follows the MD as seen from the deformation plot in Fig. 3(a).

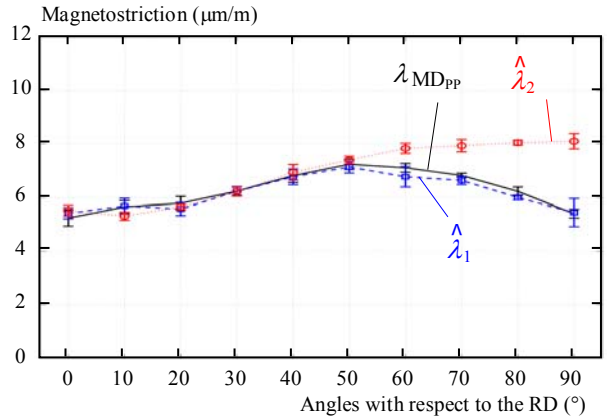

Fig. 4. $\lambda_{MD_{PP}}$, $\hat{\lambda}_1$ and $-\hat{\lambda}_2$ of the 0.35 mm thick disc sample at 1.50 T versus θ

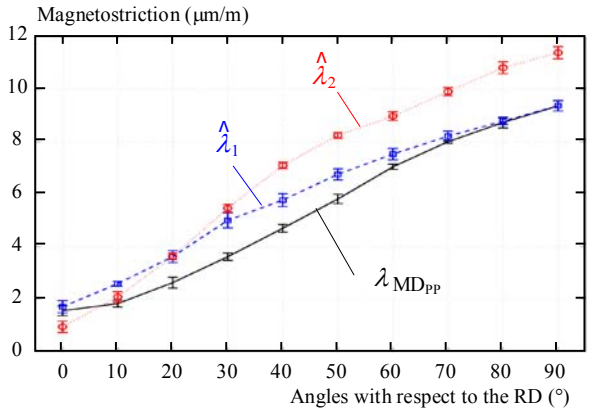

Fig. 5. $\lambda_{MD_{PP}}$, $\hat{\lambda}_1$ and $-\hat{\lambda}_2$ of the 0.50 mm thick disc sample at 1.50 T versus θ

$\lambda_{MD_{PP}}$ along the RD and TD of the Epstein strips of the 0.35 mm thick steel are compared with those measured in the disc sample in Fig. 6. Fig. 7 displays the angular characteristic of $\lambda_{MD_{PP}}$ of the 0.50 mm thick Epstein and disc specimens at peak flux densities of 1.00 T and 1.70 T respectively.

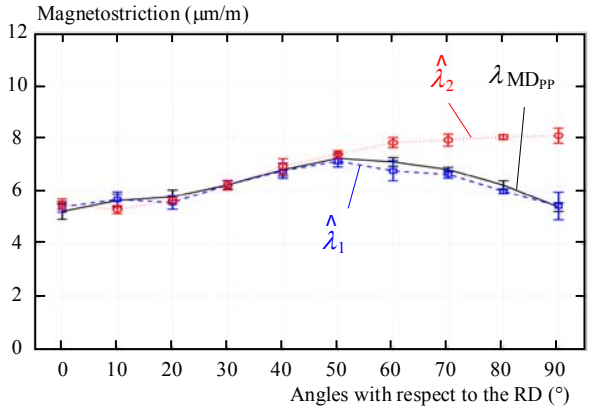

Fig. 6. Comparison of $\lambda_{MD_{PP}}$ measured in Epstein and disc samples of the 0.35 mm thick NO steel

4 ANALYSIS AND DISCUSSION

4.1 Magnetostriction measured in disc samples

The deformation plot of the 0.50 mm thick steel in Fig. 3(b) shows an intrinsic magnetostrictive anisotropy of this material. It has been described in our previous work [9] that the magnetostriction principal axis of this material tries to stay close to the TD because of the anisotropy. This can be clearly observed if the magnetisation vector rotates in the sheet plane. In addition, $\hat{\lambda}_1$ equals $\lambda_{MD_{PP}}$ at $\theta = 90°$ in Fig. 5 which also indicates that the magnetostriction principal axis prefers the TD. In contrast, $\hat{\lambda}_1$ of the 0.35 mm thick steel is very close to its $\lambda_{MD_{PP}}$ at any magnetisation angle as shown in Fig. 4 because this material is quite isotropic. This also corresponds to the deformation plot in Fig. 3 (a). Although the nominal losses of thin material grades are expected to be more anisotropic than thicker NO steels [6], textures due to different manufacturing processes play an important role in anisotropy [10]. Also, the anisotropy constant decreases as the silicon content increases [11], which could provide less magnetostrictive anisotropy in materials having high silicon content such as the 0.35 mm thick steel.

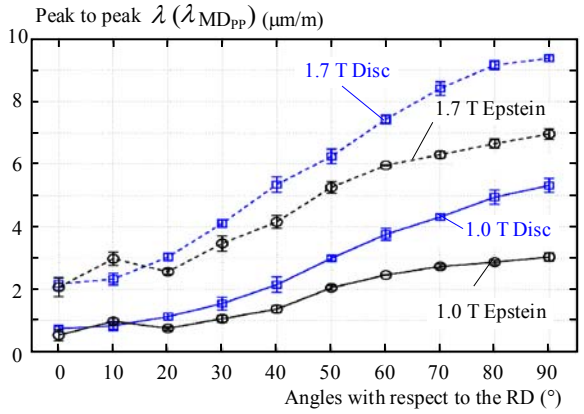

Fig. 7. Comparison of $\lambda_{MD_{PP}}$ measured in Epstein and disc samples of the 0.50 mm thick NO steel

At $\theta = 90°$, both materials expand along the TD and largely contract along the RD, which can be observed from the values of $\hat{\lambda}_1$ and $\hat{\lambda}_2$ in Fig. 4 and Fig. 5. This exhibits a magnetostriction characteristic of GO electrical steel magnetised along the TD. This can be illustrated by the schematic diagram of magnetostriction components of an ideal GO steel (only bar domains are considered) calculated from the saturation magnetostriction equation, also know as Becker-Döring equation [12]. At the demagnetised state, domains of GO steel are by definition saturated along the RD (either along the [100] or $[\bar{1}00]$ directions). The measured magnetostriction components are obtained from the differences of magnetostriction before and after magnetisation as shown in Fig. 8, which are $\lambda_x = -3\boldsymbol{\lambda}_{100}/2$ and $\lambda_y = 3(\boldsymbol{\lambda}_{100} + \boldsymbol{\lambda}_{111})/4$, where $\boldsymbol{\lambda}_{100}$ and $\boldsymbol{\lambda}_{111}$ are the magnetostriction constants. For 3% Si GO steel, $\boldsymbol{\lambda}_{100}$=23.7 μm/m and $\boldsymbol{\lambda}_{111}$=-4.1 μm/m [12], resulting in λ_{RD}=-35.55 μm/m and λ_{TD}=14.7 μm/m. The contractions of both NO materials at θ=90° are larger than their elongations, which is similar to GO steel but less pronounced.

4.2 Differences measured in Epstein samples and discs

Differences of $\lambda_{MD_{PP}}$ measured in the Epstein and disc samples are found in both steels. There are two possible causes of these differences: magnetostriction measurement techniques and the effect of sample shape.

It is apparent that $\lambda_{MD_{PP}}$ measured in an Epstein strip is the bulk magnetostriction that averages over its length, while $\lambda_{MD_{PP}}$ measured in the disc sample is the localised value. The difference between the bulk and localised

magnetostriction in Epstein strips of conventional GO electrical steel was studied by Anderson et al [13]. For the stress free condition, it showed that localised $\lambda_{MD_{PP}}$ at three positions along the Epstein strips measured by 20

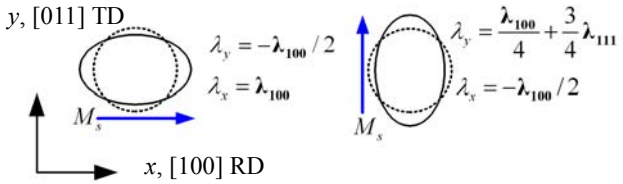

Fig. 8. Schematic diagram of magnetostriction components calculated from a single crystal of a Goss-textured GO steel (bar domains) at the demagnetised state and magnetisation along the TD

mm long resistance strain gauges were almost the same and very close to the bulk value measured by piezoelectric accelerometers. Assuming that the average grain diameter of the NO steel is around 100 μm, each strain gauge covered about 60 grains, which was considerably more than those in the GO material. Hence, the magnetostriction measurement technique would not be affected by grain to grain variation of $\lambda_{MD_{PP}}$.

Chikazumi [12] describes the form effect giving rise to spontaneous magnetostriction of an ellipsoid of rotation magnetised along its length shown in Fig. 9 (a). To minimise the total energy, the demagnetisation factor should be decreased to reduce the magnetostatic energy E_N by elongating the ellipsoid. As a result, spontaneous magnetostriction ε_{xx} is increased whereas ε_{yy} and ε_{zz} are decreased as follows

$$\varepsilon_{xx} = \frac{2\ln(2k-3)}{\ln(2k-1)} \cdot \frac{N_0}{c_{11}-c_{12}} \cdot \frac{J^2}{2\mu_0} \tag{3}$$

$$\varepsilon_{yy} = \varepsilon_{zz} = -\varepsilon_{xx}/2 \tag{4}$$

where N_0 is the initial demagnetisation factor, k is the axis ratio of the ellipsoid, μ_0 is the permeability of free space, c_{11} and c_{12} are the elastic moduli [12].

The RD of the 0.50 mm thick steel is favoured, which is quite similar to the GO steel. Thus, the 0.50 mm thick disc sample can be equivalent to an ellipse shown in Fig. 9 (b). E_N due to the magnetic anisotropy is highest when magnetised along the TD. Thus, rise of magnetostriction along the TD due to the form effect is much larger than that along the RD. On the other hand, the 0.35 mm thick steel is quite isotropic and there is no explicit easy magnetisation direction in the disc form. As a result, its geometry-dependent magnetostriction is more complicated than that of the 0.50 mm thick steel. The form effect is negligible in Epstein samples because long and narrow shape overshadows the magnetic anisotropy.

5 CONCLUSION

The direction of maximum magnetostriction of an Epstein strip of NO electrical steel is not necessarily along the strip length if the material is anisotropic. Magnetostriction measured in disc samples magnetised in a 2D magnetisation system is more convenient and requires a smaller amount of expensive material. However, sample shape could induce higher magnetostriction and magnetostrictive anisotropy in a disc sample or wide strip due to the magnetic anisotropy. Thus, magnetostriction characterised in Epstein samples may cause large errors in calculation of deformation and vibration in large electrical machine cores. Geometry-dependent magnetostriction should be investigated as it could be very important for electrical machine designers.

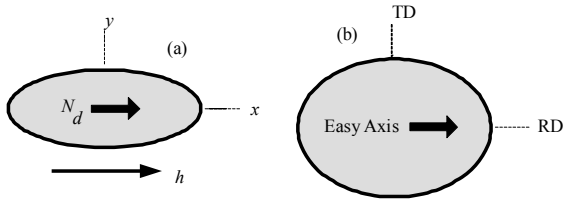

Fig. 9. (a) - Demagnetisation factor in an ellipsoid of rotation [12], (b) - Equivalent shape of the 0.50 mm disc sample due to the magnetic anisotropy

REFERENCES

[1] MOHAMMED, O. A. – CALVERT, T. – McCONNELL, R.: Coupled magnetoelastic finite element formulation including anisotropic reluctivity tensor and magnetostriction effects for machinery applications, IEEE Trans. Magn. **37** (2001), 3388–3392

[2] HUBER, O. – DANIEL, L. – BILLARDON, R.: Experimental analysis of the magnetoelastic anisotropy of a non-oriented silicon iron alloy, J. Magn. Magn. Mater. **254-255** (2003), 352–354

[3] SOMKUN, S. – MOSES, A. J. – ANDERSON, P. I.: Effect of magnetostriction anisotropy in nonoriented electrical steels on deformation of induction motor stator cores, IEEE Trans. Magn. **45** (2009), 4744–4747

[4] NENCIB, S. – SPORNIC, S. – KEDOUSLEBOUC, A. – CORNUT, B.: Macroscopic anisotropy characterization of Sife using a rotational single sheet tester, IEEE Trans. Magn. **31** (1995), 4047-4049

[5] MOSES, A. J.: Measurement and analysis of magnetic fields on the surface of grain-oriented silicon steel sheet," J. Phys. IV **08** (1998), Pr2-561-Pr2-565

[6] British Standard: BS EN10106:2007 Cold Rolled Non-oriented Electrical Steel Sheet and Strip Delivered in the Fully Processed State, 2007

[7] KLIMCZYK, P.: Influence of Cutting Techniques on Magnetostriction Measured in Epstein Strips of Electrical Steel Sheets, Unpublished document, Wolfson Centre for Magnetics, Cardiff University, 2010.

[8] KLIMCZYK, P. – MOSES, A. J. – ANDERSON, P. I. – DAVIES, M.: Challenges in magnetostriction measurements under stress, Prz. Elektrotechniczny **85** (2009), 100-102

[9] SOMKUN, S. – MOSES, A. J. – ANDERSON, P. I. – KLIMCZYK, P.: Magnetostriction anisotropy and rotational magnetostriction of a nonoriented electrical steel, IEEE Trans. Magn. **46** (2010), 302-305

[10] SHIOZAKI, M. – KUROSAKI, Y.: Anisotropy of magnetic properties in non-oriented electrical steel sheets, Texture. Microstruct. **11** (1989), 159-170

[11] MOSES, T.: Opportunities for exploitation of magnetic materials in an energy conscious world, Interdiscipl. Sci. Rev. **27** (2002), 100-113

[12] CHIKAZUMI, S.: Physics of Magnetism, John Wiley & Sons, New York, 1964.

[13] ANDERSON, P. I. – MOSES, A. J. – STANBURY, H. J.: Evaluation of magnetostriction measurement techniques, Non Linear Electromagnetic Systems, **13** (1998), 341-344

Received November 2010